Hindawi Publishing Corporation
Mathematical Problems in Engineering
Volume 2014, Article ID 713678, 9 pages
http://dx.doi.org/10.1155/2014/713678

Research Article

An Analytical Model for Fatigue Crack Propagation Prediction with Overload Effect

Shan Jiang, Wei Zhang, Xiaoyang Li, and Fuqiang Sun

Science and Technology on Reliability and Environmental Engineering Laboratory, School of Reliability and Systems Engineering, Beihang University, Beijing 100191, China

Correspondence should be addressed to Wei Zhang; zhangwei.dse@buaa.edu.cn

Received 2 May 2014; Revised 22 June 2014; Accepted 23 June 2014; Published 23 July 2014

Academic Editor: Xuefeng Chen

Copyright © 2014 Shan Jiang et al. This is an open access article distributed under the Creative Commons Attribution License, which permits unrestricted use, distribution, and reproduction in any medium, provided the original work is properly cited.

In this paper a theoretical model was developed to predict the fatigue crack growth behavior under the constant amplitude loading with single overload. In the proposed model, crack growth retardation was accounted for by using crack closure and plastic zone. The virtual crack annealing model modified by Bauschinger effect was used to calculate the crack closure level in the outside of retardation effect region. And the Dugdale plastic zone model was employed to estimate the size of retardation effect region. A sophisticated equation was developed to calculate the crack closure variation during the retardation area. Model validation was performed in D16 aluminum alloy and 350WT steel specimens subjected to constant amplitude load with single or multiple overloads. The predictions of the proposed model were contrasted with experimental data, and fairly good agreements were observed.

1. Introduction

The damage tolerance concept is widely used in modern aircraft design to ensure flight safety, which has made the prediction of fatigue crack propagation lives of aircraft components under service loading necessary [1, 2]. In 1860s, Paris and Erdogan [3] proposed a fracture mechanics based method for fatigue life prediction, which correlated the fatigue crack growth rate to the applied stress intensity factor range. One issue of Paris' model is that the stress ratio effect is not considered. Many modifications of Paris' law have been proposed in the literatures [4–6], one of the most important modifications being the inclusion of the crack closure concept. Crack closure was first introduced into the fatigue crack growth analysis by Wolf [4]. And then, plenty of research has been done concerning the crack closure using experimental investigation, numerical analysis, and theoretical studies [7–16]. Zhang and Liu [7, 8] performed a state-of-the-art in situ SEM testing to investigate fatigue crack growth behavior continuously within a load cycle. In their study, crack closure's existence and its influence on crack propagation was directly observed. Newman [9, 10] used a strip yield model to analyze the crack closure problems. Budiansky and Hutchinson [13] proposed a method to estimate the crack closure caused by plasticity in plane stress cases under constant cyclic loading. The crack closure models reviewed above can eliminate stress ratio R effect and describe fatigue crack behavior under constant amplitude loading well. However, since crack closure calculation involves the highly nonlinear analysis of cyclic plasticity and contact analysis, direct tracking of crack closure under a variable amplitude loading is extremely difficult and of high computational cost. So, the plastic zone concept is also employed to describe the crack growth behavior under general loading conditions. Willenborg et al. and Wheeler [17, 18] proposed a series of models to analyze the fatigue crack growth under variable loading cases. In their papers, the plastic zone concept was used to explain the overload retardation effect. Plentiful literatures were presented to investigate fatigue crack growth behavior with the single overload [19–22], and many modifications have been proposed to correlate experimental observations. However, in most of these models, empirical coefficients are added to match the testing data under the influence of retardation, instead of modeling directly based on the mechanisms, such as the crack closure. Moreover, the recent in situ SEM experimental observations have shown that

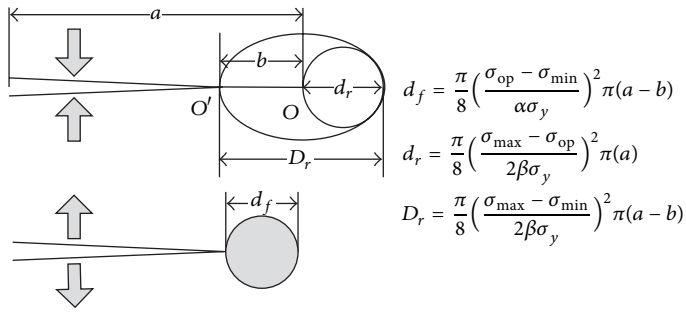

Figure 1: Schematic illustration of real crack and virtual crack model.

single overload has a significant impact on the crack closure within the large plastic zone [23]. Therefore, crack closure variation is probably a good explanation of the retardation phenomenon. In this paper, a mechanism-based method will be developed to predict fatigue crack growth behavior under the single overload, in which crack closure and plastic zone concept are considered.

The paper is organized as follows. First, the fatigue crack growth model and the modified virtual crack annealing crack closure model are briefly reviewed. Second, our proposed model for crack growth retardation behavior estimation is discussed in detail. The model is derived based on plastic zone and crack closure variation. And then model validation is performed using the experimental data in D16 aluminum alloy and 350WT steel from the literature. Finally, some conclusions and future work are given based on the current study.

2. Methodology Development

A general fatigue crack growth model can be expressed as (1) by Wolf [4]. The fatigue crack growth rate is determined by the effective stress intensity factor range

$$\frac{da}{dN} = C\left(\Delta K_{\text{eff}}\right)^m, \qquad \Delta K_{\text{eff}} = K_{\max} - K_{\text{op}}, \tag{1}$$

where da/dN is the crack growth rate, ΔK_{eff} is the effective stress intensity factor, $K_{\max}$ is the stress intensity factor of the peak load, and K_{op} is the crack closure level; C, m are calibration parameters.

In this paper the virtual crack annealing model is employed to avoid considering the complex contact of crack closure [7]. This analytical closure model is based on plasticity ahead of crack tip, but it does not consider the Bauschinger effect. So a brief derivation of the modified closure model is discussed in the following part.

As shown in Figure 1, in the process of unloading, when the stress level decreases from $\sigma_{\max}$ to σ_{op}, a reversed plastic zone with diameter d_r appears ahead of the real crack tip "O". And as the stress level continues reducing from σ_{op} to $\sigma_{\min}$, the crack tip will fully close and the reversed plastic zone remains constant due to the crack closure. According to the assumption of crack annealing, the closed part that has the length of "b" can be considered as nonfractured material. So, there is an equivalent reversed plastic zone with diameter D_r, and the virtual crack tip position is O'. In the following loading process, when the stress level increases from $\sigma_{\min}$ to σ_{op}, the superposition of the stress within the forward plastic zone with diameter d_f and the residual stress within the distance "b" ahead of the virtual crack is zero and the crack tip opens. So, the equation $d_f = D_r - d_r$ can be established. Additionally, for anisotropic materials, the Bauschinger effect has a significant impact on the cyclic plastic deformation ahead of crack tip. Thus, equation can be expressed as

$$\frac{\pi}{8}\left(\frac{\sigma_{\max}-\sigma_{\min}}{2\beta\sigma_y}\right)^2\pi(a-b) - \frac{\pi}{8}\left(\frac{\sigma_{\max}-\sigma_{\text{op}}}{2\beta\sigma_y}\right)^2\pi(a) = \frac{\pi}{8}\left(\frac{\sigma_{op}-\sigma_{\min}}{\alpha\sigma_y}\right)^2\pi(a-b), \tag{2}$$

where σ_y is tensile yield strength, $\sigma_{\max}$ is maximum stress level, $\sigma_{\min}$ is minimum stress level, σ_{op} is stress level of crack opening, α is the Bauschinger effect factor in loading process, and β is the Bauschinger effect in unloading process.

Since the crack overlapping length is very small compared with the true crack length (i.e., $b \ll a$), its effect on the stress intensity factor calculation can be ignored. Equation (2) can be rewritten as

$$\begin{aligned}&\left(\alpha+4\beta^2\right)\sigma_{\text{op}}^2 - \left(8\beta^2\sigma_{\min}+2\alpha^2\sigma_{\max}\right)\sigma_{\text{op}} + \left(4\beta^2\sigma_{\min}^2+2\alpha^2\sigma_{\max}\sigma_{\min}-\alpha^2\sigma_{\min}^2\right)=0,\\ &\left(1+4\gamma^2\right)\sigma_{\text{op}}^2 - \left(8\gamma^2\sigma_{\min}+2\sigma_{\max}\right)\sigma_{\text{op}} + \left(4\gamma^2\sigma_{\min}^2+2\sigma_{\max}\sigma_{\min}-\sigma_{\min}^2\right)=0,\end{aligned} \tag{3}$$

where γ is equal to β/α. Equation (3) is the general solution using the virtual crack annealing model for the crack opening stress calculation under constant amplitude loadings. Equation (3) can be further simplified as

$$\left(\sigma_{\text{op}}-\sigma_{\min}\right)\left[\left(1+4\gamma^2\right)\sigma_{\text{op}} - 2\sigma_{\max} - \left(4\gamma^2-1\right)\sigma_{\min}\right] = 0. \tag{4}$$

There are two possible solutions for the opening stress level under the proposed virtual crack annealing model. One

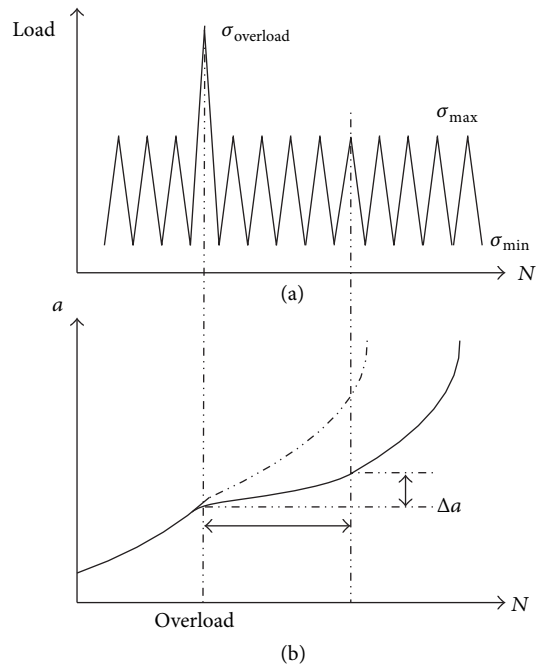

Figure 2: Schematic illustration of CA load interspersed with single-cycle tensile overload.

solution is $\sigma_{op} = \sigma_{min}$, which indicates that there is no crack closure and the overlapped length is zero. The other solution is $\sigma_{op}/\sigma_{max} = (1/(1 + 4\gamma^2))[2 + (4\gamma^2 - 1)R]$. This observation indicates that either there is no crack closure or there is a unique crack closure level under constant amplitude loadings. In this paper, the modified virtual crack annealing model is used to make predictions of the fatigue crack growth behavior in the outside of retardation effect region.

Retardation caused by overloads is a typical phenomenon of loading interaction effect. A great number of papers were presented to investigate the single overload [24–28]. Generally, overloads will induce large plastic deformation ahead of the crack tip and retard the crack growth rate in the subsequence loading of a certain range. As the developing of the crack, the retardation effect gradually recedes. When the crack grows beyond the large plastic zone, the retardation effect vanishes completely. Before the crack growth rate decreases, there is an accelerated crack growing stage, which has been termed delayed retardation. That transient acceleration right after overload is small enough to be neglected in this investigation. As it is shown in Figure 2, the crack growth length is "Δa" under the influence of a single overload.

The crack growth behavior is shown in Figure 3. After the overload, the crack growth rate increases transitorily and then decreases sharply. Once the da/dN value reaches to minimum, crack growth rate increases gradually and finally recovers to the equilibrium constant amplitude loading growth rate.

The crack tip plastic zone associated with the application of a single overload is shown in Figure 4(a). A new approach to estimation of crack opening stress under the influence of single overload is proposed, as shown in Figure 4(b). When

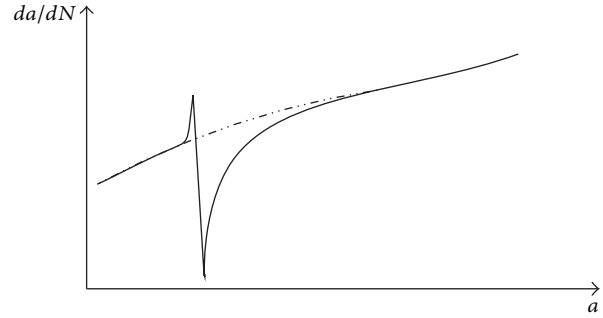

Figure 3: Schematic of delayed retardation due to single tensile overload.

the crack grows to point O_1, a single overload stress is applied and a large plastic zone appears ahead of the crack tip. As the crack penetrates into this plastic zone and grows to point O_3, the retardation effect gradually recedes until it vanishes.

A function of σ_{op}/σ_{max} and the crack length is established to calculate the crack closure variation during the retardation region, which is shown in Figure 4(b). The points C and D in this figure, respectively, represent the situation of crack growing to points O_1 and O_3 in Figure 4(a). Equation (5) can be obtained based on the modified virtual crack annealing model above:

$$Y_C = \left(\frac{\sigma_{op}}{\sigma_{max}}\right)_C = \frac{2}{1+4\gamma^2} + \frac{4\gamma^2 - 1}{1+4\gamma^2} \times \frac{R}{R_{ol}}, \quad (5)$$

where γ is Bauschinger effect factor, R is the load ratio, and R_{ol} is the overload ratio. The left side of (5) is the ordinate of point C. Similarly, the ordinate of point D can be illustrated by the following:

$$Y_D = \frac{2}{1+4\gamma^2} + \frac{4\gamma^2 - 1}{1+4\gamma^2} \times R. \quad (6)$$

The horizontal ordinate of point D is

$$X_D = a_0 + D_m, \quad (7)$$

where a_0 is the horizontal ordinate of point C, which is the crack length when single overload is applied. D_m is the diameter of plastic zone created by that single overload. If point D is considered to be the ordinate origin, the equation of the curve between points C and D is

$$f(x) = \frac{Y_C - Y_D}{(X_C)^n} \cdot (-x)^n, \quad (8)$$

where Y_C and Y_D are, respectively, the ordinate of points C and D and X_C is the horizontal ordinate of point C. When the value of n can be 2, 1, and 0.5, the curve is, respectively, shown as (A), (B), and (C) in Figure 4. Based on the current study, $n = 1$ is a good approximation for aluminum alloy. If the O is considered to be the ordinate origin, (7) can be rewritten as

$$f(x) = Y_D + \frac{Y_C - Y_D}{(X_C - X_D)^n}\left((X_C + D_m) - x\right)^n. \quad (9)$$

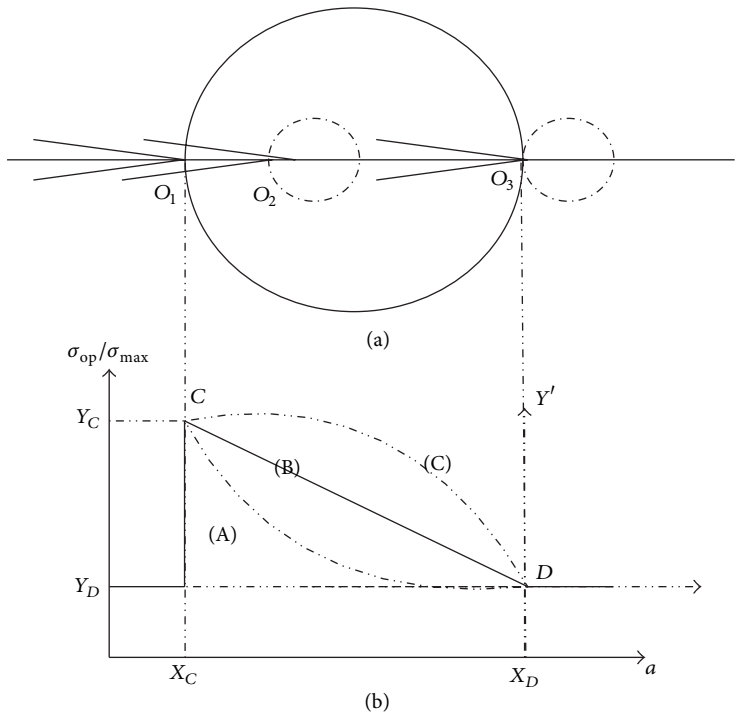

Figure 4: (a) Crack-tip plastic zone due to single tensile overload; (b) the mathematical derivation of σ_{op} based on crack closure model.

Based on the discussion above, the new crack closure model is established as (10), which is used to describe fatigue crack propagation behavior under single overload interspersed in a constant amplitude loading spectrum. Consider

$$\sigma_{op} = \begin{cases} \dfrac{1}{4\gamma^2+1}\left(\left(4\gamma^2-1\right)\sigma_{min}+2\sigma_{max}\right) \\ \qquad \text{before single overload} \\ \dfrac{1}{4\gamma^2+1}\left(\left(4\gamma^2-1\right)\sigma_{min}+2\sigma_{ol}\right) \\ \qquad \text{single overload} \\ \left(\dfrac{2}{1+4\gamma^2}+\dfrac{4\gamma^2-1}{1+4\gamma^2}\times R\right) \\ \quad +\dfrac{\left(\left(4\gamma^2-1\right)/\left(1+4\gamma^2\right)\right)\left(\left(R/R_{ol}\right)-R\right)}{\left(-D_m\right)^n} \\ \quad \times\left(a_0+D_m-a\right)^n \\ \qquad \text{under influence of single overload} \\ \dfrac{1}{4\gamma^2+1}\left(\left(4\gamma^2-1\right)\sigma_{min}+2\sigma_{max}\right) \\ \qquad \text{after influence of single overload.} \end{cases} \tag{10}$$

The cycle by cycle algorithm is used to implement the above model. The flow chart for fatigue crack growth prediction based on the modified crack closure model is shown in Figure 5.

Table 1: Standard chemical composition [28].

Chemical composition of D16 aluminum alloy						
Element	Cu	Mg	Mn	Si	Fe	Zn
Weight %	3.8–4.9	1.2–1.8	0.3–0.9	0.5	0.5	0.3

3. Experimental Validation

3.1. Crack Growth Predictions in D16 under Constant Loading and Single Overload. The experimental data for model validation are from the literature [27, 28]. The material used in both papers was D16 aluminum alloy. The standard chemical composition is shown in Table 1. And the mechanical properties of this material in longitudinal (LT) orientation were as follows: $\sigma_y = 347$ MPa, $K_c = 40 \sim 45$ MPa$*$m$^{0.5}$, and percentage elongation = 12%.

Before any predictions can be made, there are several unknown parameters (see (1) and (10)) that need to be calibrated. Three sets of $da/dN \sim dK$ testing data are used to evaluate these parameters (Figure 6), which are assumed to depend on the material only [27]. The calibrated parameters are $m = 2.4534$ and $C = 1.2331$E-9, and Bauschinger effect factor γ is 0.97.

Then additional two sets of a-N data are used to validate the proposed model. The specimen configuration for these tests is [27] width = 100 mm, length = 500 mm, and thickness = 4 mm. Initial half crack length is $a = 5.0$ mm. The specimen was subjected to a constant amplitude load sequence with $\sigma_{max} = 64$ MPa, $R = 0$. And the overload ratio is 2.

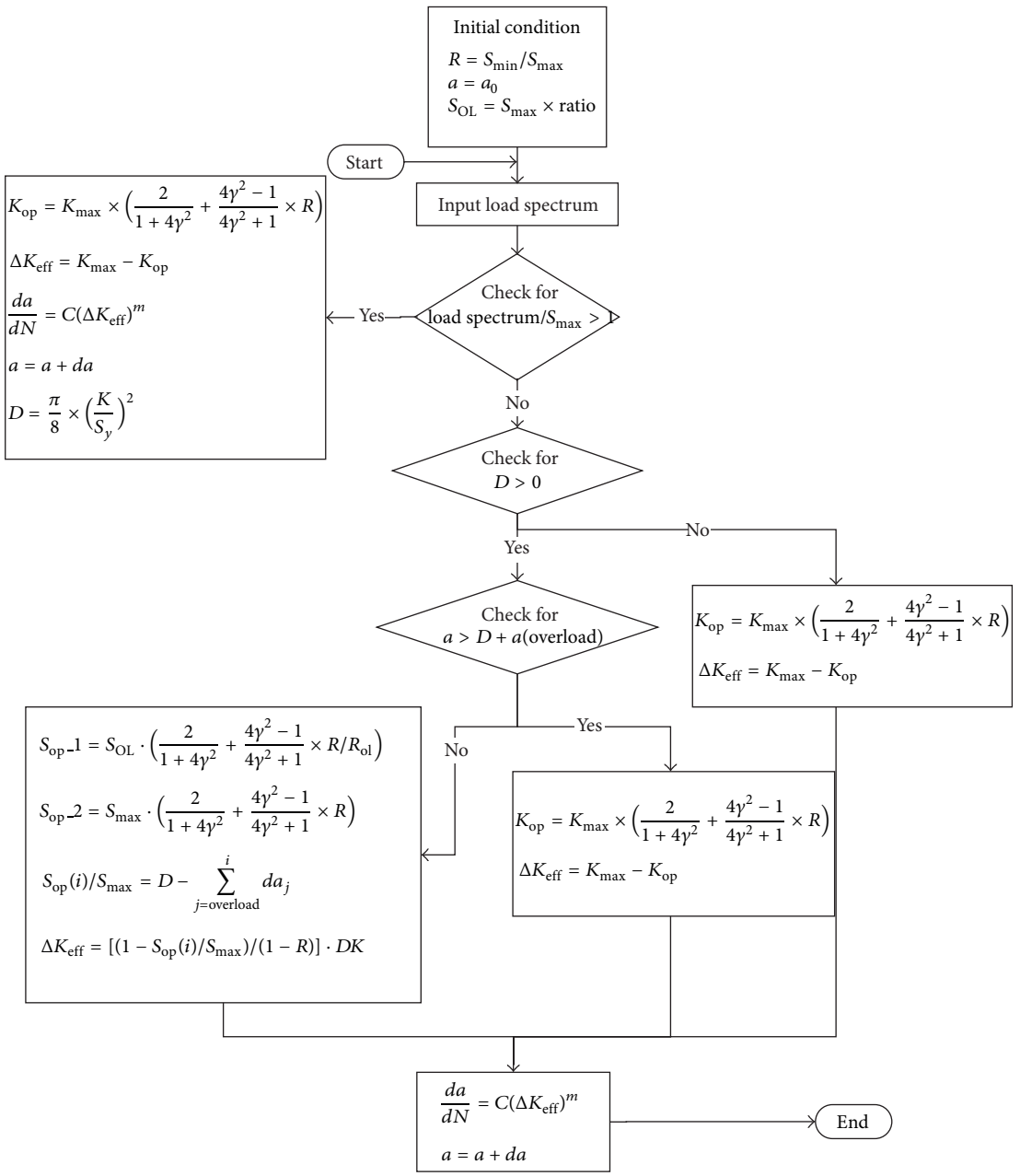

Figure 5: Flow chart for fatigue crack growth calculation.

The model predictions are compared to the experimental data in Figure 7. The x-axis is the number of cycles, and the y-axis is crack length. The red circlets represent the fatigue crack growth under the constant amplitude loading; and the small blue squares are the counterpart under the constant amplitude load with single overload. It is observed that the predictions by proposed model match the testing data well.

More detailed information can be obtained in the da/dN-a curve in Figure 8. Right after the single overload, the fatigue crack growth rate increases in a short time and then decreases sharply. After a certain crack length, the retardation phenomenon vanishes and the crack growth rate turns back to the original trend. Note that very good agreement is observed between the model prediction and experimental data.

Additional set of testing data is used for the model validation in the same material and similar specimen configuration [28]. Specimen dimensions are as follows: length = 180 mm, width = 45 mm, and thickness = 1.5 mm. Initial crack length is $a = 4.0$ mm. The specimens are subjected to two different loading spectra: (1) constant amplitude loading with no overloads ($\sigma_{max} = 60$ MPa, $R = 0.1$) and (2) constant amplitude load with single overload applied at the certain crack length (overload ratio is 2) [28]. Following the same procedure, the comparisons between predictions and experimental data are shown in Figure 9. Under the

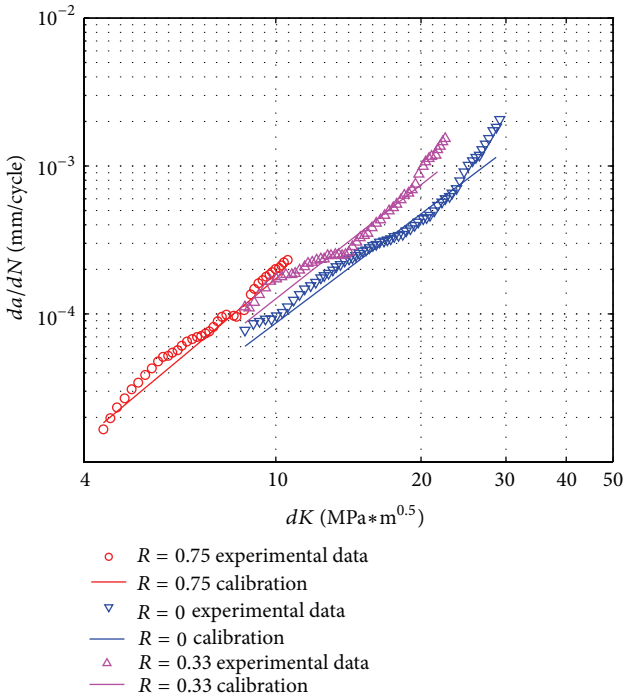

Figure 6: da/dN-dK calibration.

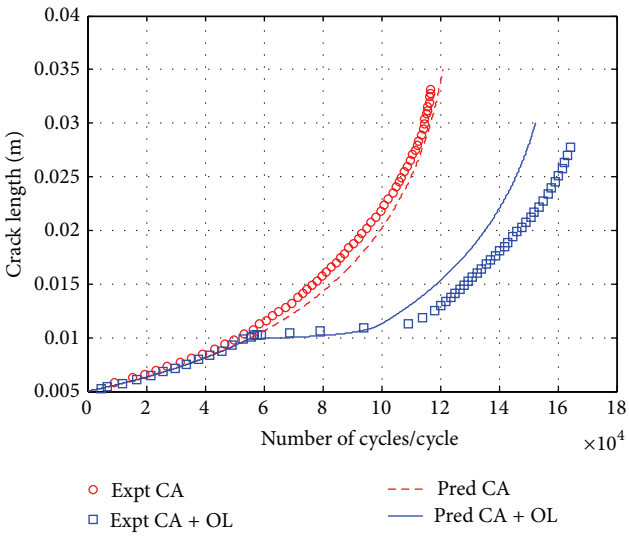

Figure 7: a-N curve for constant amplitude and single overload cases.

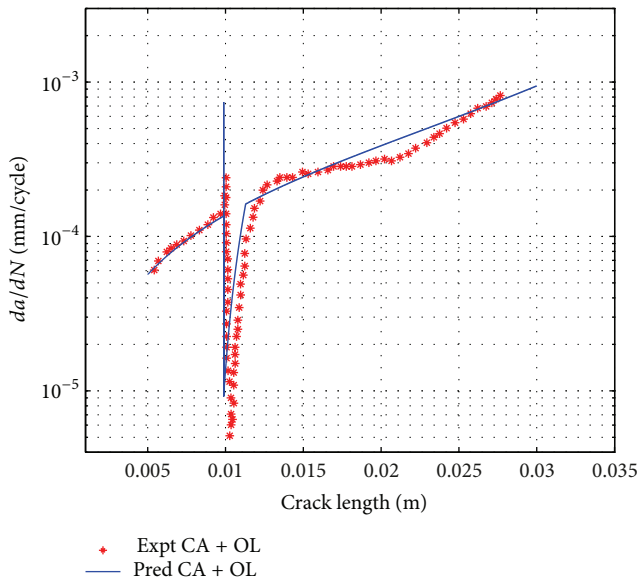

Figure 8: da/dN-a curve for constant amplitude and single overload cases.

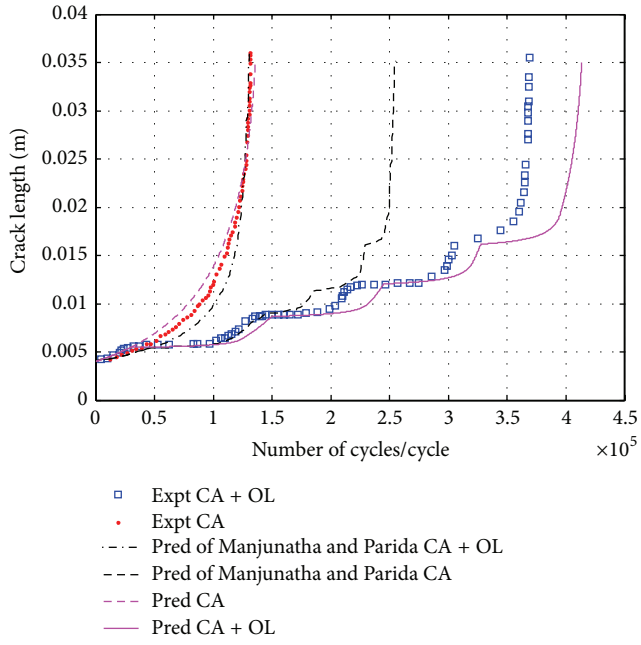

Figure 9: a-N periodic spike loading.

former loading spectrum, both of our proposed model and Manjunatha's model can give very good predictions [28]. In the latter loading case, the single overloads are applied at the crack length of 5.5, 9, 12, and 16 mm, respectively. The prediction of our proposed model is just slightly slower than the experimental data, while Manjunatha's prediction is much faster than that of the experimental data. The fatigue life ratios expressed as $N_{\text{expt}}/N_{\text{pred}}$ are, respectively, calculated to be 0.89 by using the proposed model and 1.44 by using Manjunatha's model. Obviously, the proposed closure based model can give the better predictions.

3.2. Crack Growth Prediction in 350WT under Constant Loading and Single Overload. In this section, the model validation will extend to 350WT steel. The experimental data are given by Taheri et al. [29]. The specimen dimensions are as follows: length = 300 mm, width = 100 mm, and thickness = 5 mm. Initial center crack length is $2a$ = 20.0 mm. Recording test data was started at crack length of 11.17 mm. In addition,

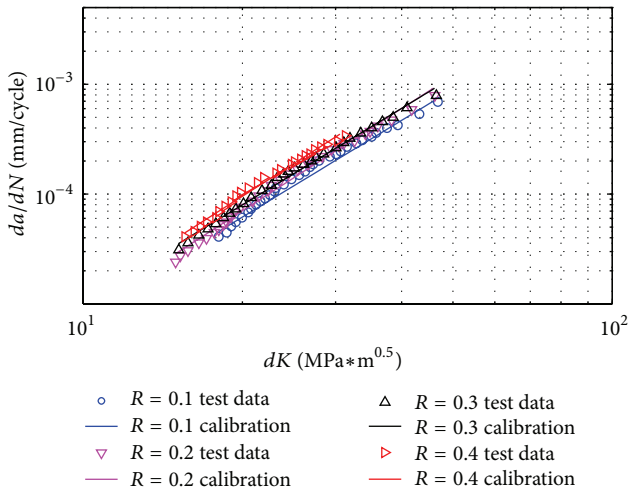

FIGURE 10: da/dN-dK calibration figure.

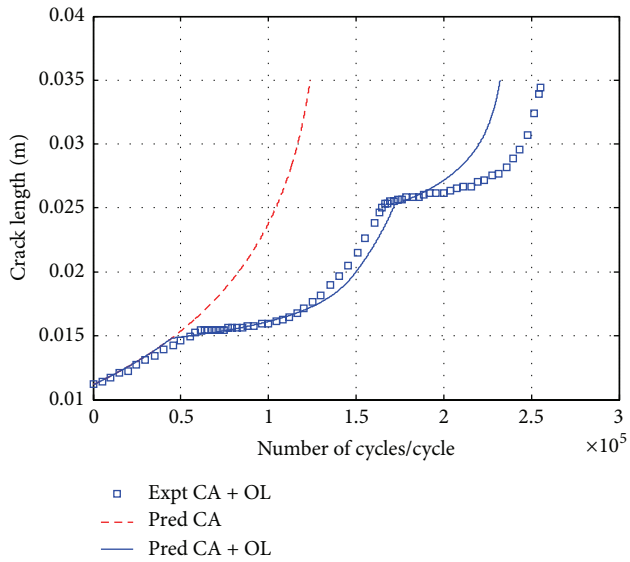

FIGURE 11: a-N curve for constant amplitude and single overload cases.

the mechanical properties of 350WT in longitudinal (LT) orientation are as follows: σ_y = 350 MPa, σ_{UTS} = 524 MPa, Modulus of elasticity = 205 GPa, and Poisson's ration = 0.30 [30].

Similarly, the parameters are calibrated by the $da/dN \sim \Delta K$ data in the literature [19], as shown in Figure 10. The fitting coefficients are $C = 4.3136E - 11$ and $m = 2.9245$, and the Bauschinger effect factor γ is 1.05.

Figure 11 shows the comparison between the predicted a-N curve and the experimental data in 350WT steel specimens. The single overloads are applied at the crack length of 15 and 25 mm. It can be seen that there are two obvious retarded regions right after the overload in the experimental data. The prediction follows almost the same trend as the experimental observation. Predicted total fatigue lives are slightly lower than the experimental values.

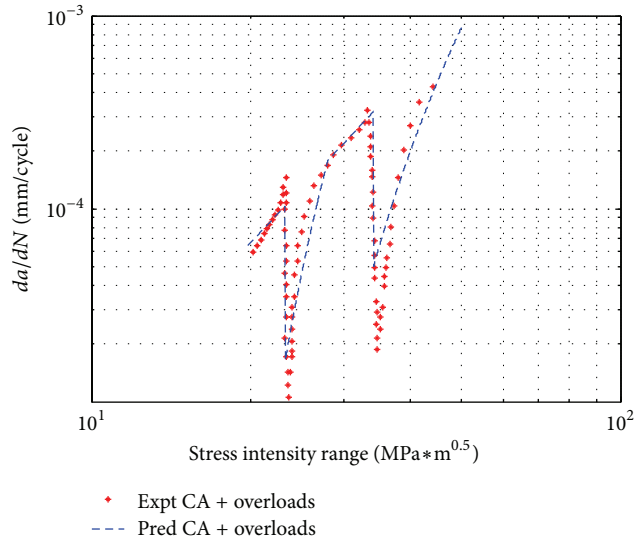

FIGURE 12: ΔK-da/dN cruve for constant amplitude and single overload cases.

In Figure 12, crack growth rate variation caused by overloads is also compared with our model prediction. It is clear that the prediction matches the experimental data very well, especially in the retardation region. Hence, it is proven that the method proposed in this paper is applicable to predict the fatigue crack growth behavior under the constant loading with single overloads in 350WT steel.

4. Conclusion

In this investigation, a theoretical model is developed to predict the fatigue crack growth behavior under the constant amplitude loading with single overload. The crack growth retardation was accounted for by using crack closure concept and plastic zone. Model was validated in D16 aluminum alloy and 350WT steel subjected to several different loading spectra, and the predictions matched experimental data well. The following conclusions can be drawn based on the current investigation.

(1) Fatigue crack growth is slowed down by application of single overload cycle. A convincing reason for this retardation phenomenon is that after the overload a large plastic zone will form ahead of the crack tip, which can increase the crack closure level within this region. And as the crack grows through the large plastic zone, the crack closure level will gradually decrease which can be described as a linear function. The retardation effects disappear after a certain characteristic crack length extension from the overload position. This extension is approximately equal to monotonic plastic zone size caused by the overload.

(2) The proposed model is derived from fatigue crack growth mechanisms (such as crack closure, plastic zone, and Bauschinger effect), and it does not require

any additional parameters which has no physical meaning.

(3) The above statement is only valid under the current investigated loading spectrums and materials. In the future, the whole frame work should be extended to other materials. Additionally, branching and bifurcation caused by overload can also retard the crack growth rate, which should be investigated in the future.

Nomenclature

a:	Crack length
Δa:	Crack growth in one cycle
da:	Infinitesimal crack increment
da/dN:	Fatigue crack growth rate per cycle
$\sigma_{\min}$, $\sigma_{\max}$:	Minimum and maximum stress in one loading cycle
σ_{op}:	Stress level at which the crack begins to grow
σ_{ol}:	Stress level of single overload
R:	Stress ratio
R_{ol}:	Overload ratio
$K_{\max}$, $K_{\min}$:	Maximum/minimum stress intensity factor
ΔK:	Stress intensity factor range
K_{op}:	Stress intensity factor at which the crack begins to grow
ΔK_{eff}:	Effective stress intensity factor range
D_m:	Monotonic plastic zone size
D_f:	Forward plastic zone size
d_r, D_r:	Reverse plastic zone size
σ_y:	Material yield strength
α:	Bauschinger effect factor in loading process
β:	Bauschinger effect factor in unloading process
γ:	Bauschinger effect factor.

Conflict of Interests

The authors declare that there is no conflict of interests regarding the publication of this paper.

Acknowledgment

The research is financially supported by the specialized research fund for the doctoral program of higher education funding under the contract no. 20131102120047.

References

[1] R. C. Alderliesten and J. J. Homan, "Fatigue and damage tolerance issues of Glare in aircraft structures," *International Journal of Fatigue*, vol. 28, no. 10, pp. 1116–1123, 2006.

[2] A. T. Kermanidis, P. V. Petroyiannis, and S. G. Pantelakis, "Fatigue and damage tolerance behaviour of corroded 2024 T351 aircraft aluminum alloy," *Theoretical and Applied Fracture Mechanics*, vol. 43, no. 1, pp. 121–132, 2005.

[3] P. Paris and F. Erdogan, "A critical analysis of crack propagation laws," *Journal of Fluids Engineering*, vol. 85, no. 4, pp. 528–533, 1963.

[4] E. Wolf, "Fatigue crack closure under cyclic tension," *Engineering Fracture Mechanics*, vol. 2, no. 1, pp. 37–45, 1970.

[5] J. C. Newman Jr., *Prediction of Crack Growth under Variable-Amplitude Loading in Thin-Sheet 2024-T3 Aluminum Alloys*, Engineering against Fatigue, University of Sheffield, 1997.

[6] W. Elbert, "The significance of fatigue crack closure," in *Damage Tolerance in Aircraft Structures: A Symposium Presented at the Seventy-Third Annual Meeting American Society for Testing and Materials*, pp. 486–230, ASTM International, Toronto, Canada, June 1971.

[7] W. Zhang and Y. Liu, "In situ SEM testing for crack closure investigation and virtual crack annealing model development," *International Journal of Fatigue*, vol. 43, pp. 188–196, 2012.

[8] W. Zhang and Y. Liu, "Investigation of incremental fatigue crack growth mechanisms using in situ SEM testing," *International Journal of Fatigue*, vol. 42, pp. 14–23, 2012.

[9] J. C. Newman Jr., "A crack-closure model for predicting fatigue crack growth under aircraft spectrum loading," *ASTM International—STP Series*, vol. 748, pp. 53–84, 1981.

[10] J. C. Newman Jr., "A crack opening stress equation for fatigue crack growth," *International Journal of Fracture*, vol. 24, no. 4, pp. R131–R135, 1984.

[11] J. Z. Zhang and P. Bowen, "On the finite element simulation of three-dimensional semi-circular fatigue crack growth and closure," *Engineering Fracture Mechanics*, vol. 60, no. 3, pp. 341–360, 1998.

[12] F. V. Antunes, A. G. Chegini, R. Branco, and D. Camas, "A numerical study of plasticity induced crack closure under plane strain conditions," *International Journal of Fatigue*, 2014.

[13] B. Budiansky and J. W. Hutchinson, "Analysis of closure in fatigue crack growth," *Journal of Applied Mechanics*, vol. 45, no. 2, pp. 267–276, 1978.

[14] J. Llorca and V. S. Gálvez, "Modelling plasticity-induced fatigue crack closure," *Engineering Fracture Mechanics*, vol. 37, no. 1, pp. 185–196, 1990.

[15] P. F. P. de Matos and D. Nowell, "Modeling fatigue crack closure using dislocation dipoles," 2006.

[16] J. H. Kim and S. B. Lee, "Behavior of plasticity-induced crack closure and roughness-induced crack closure in aluminum alloy," *International Journal of Fatigue*, vol. 23, supplement 1, pp. S247–S251, 2001.

[17] J. Willenborg, R. M. Engle, and H. A. Wood, "A crack growth retardation model using an effective stress concept," Tech. Rep., 1971.

[18] O. E. Wheeler, "Spectrum loading and crack growth," *Journal of Basic Engineering Transactions of the ASME*, vol. 94, no. 1, pp. 181–186, 1972.

[19] X. Huang, M. Torgeir, and W. Cui, "An engineering model of fatigue crack growth under variable amplitude loading," *International Journal of Fatigue*, vol. 30, no. 1, pp. 2–10, 2008.

[20] S. Daneshpour, M. Koçak, S. Langlade, and M. Horstmann, "Effect of overload on fatigue crack retardation of aerospace Al-alloy laser welds using crack-tip plasticity analysis," *International Journal of Fatigue*, vol. 31, no. 10, pp. 1603–1612, 2009.

[21] B. K. C. Yuen and F. Taheri, "Proposed modifications to the Wheeler retardation model for multiple overloading fatigue life

prediction," *International Journal of Fatigue*, vol. 28, no. 10, pp. 1803–1819, 2006.

[22] F. J. McMaster and D. J. Smith, "Predictions of fatigue crack growth in aluminium alloy 2024-T351 using constraint factors," *International Journal of Fatigue*, vol. 23, no. 1, pp. S93–S101, 2001.

[23] J. Yang, W. Zhang, and Y. Liu, "Existence and insufficiency of the crack closure for fatigue crack growth analysis," *International Journal of Fatigue*, vol. 62, pp. 144–153, 2013.

[24] K. Sadananda, A. K. Vasudevan, R. L. Holtz, and E. U. Lee, "Analysis of overload effects and related phenomena," *International Journal of Fatigue*, vol. 21, no. 1, pp. S233–S246, 1999.

[25] Y. K. Tür and Ö. Vardar, "Periodic tensile overloads in 2024-T3 AL-alloy," *Engineering Fracture Mechanics*, vol. 53, no. 1, pp. 69–77, 1996.

[26] S. Daneshpour, J. Dyck, V. Ventzke, and N. Huber, "Crack retardation mechanism due to overload in base material and laser welds of Al alloys," *International Journal of Fatigue*, vol. 42, pp. 95–103, 2012.

[27] J. Schijve, M. Skorupa, A. Skorupa, T. Machniewicz, and P. Gruszczynski, "Fatigue crack growth in the aluminium alloy D16 under constant and variable amplitude loading," *International Journal of Fatigue*, vol. 26, no. 1, pp. 1–15, 2004.

[28] C. M. Manjunatha and B. K. Parida, "Prediction of fatigue crack growth after single overload in an aluminum alloy," *AIAA Journal*, vol. 42, no. 8, pp. 1536–1542, 2004.

[29] F. Taheri, D. Trask, and N. Pegg, "Experimental and analytical investigation of fatigue characteristics of 350WT steel under constant and variable amplitude loadings," *Marine Structures*, vol. 16, no. 1, pp. 69–91, 2003.

[30] P. A. Rushton and F. Taheri, "Prediction of crack growth in 350WT steel subjected to constant amplitude with over- and under-loads using a modified wheeler approach," *Marine Structures*, vol. 16, no. 7, pp. 517–539, 2003.

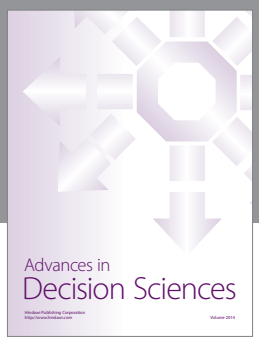

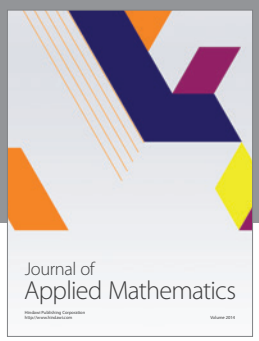

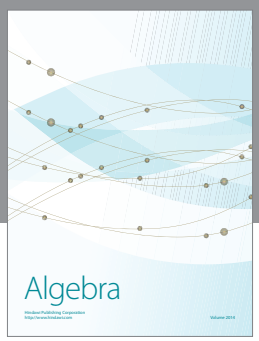

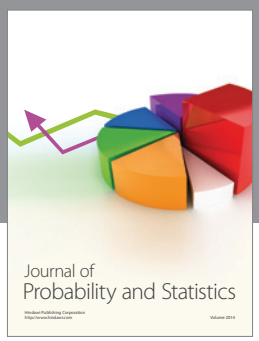

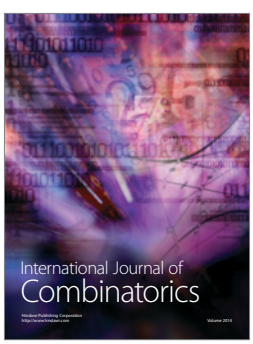

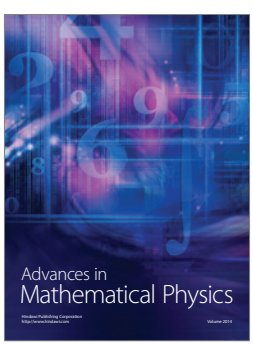

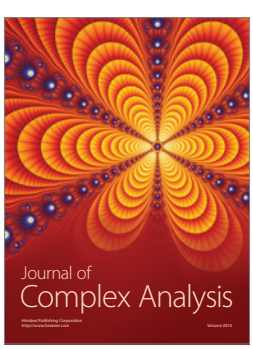

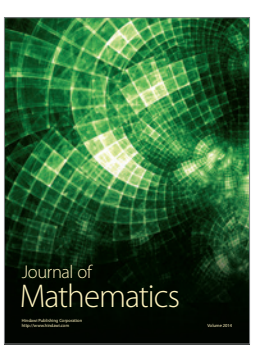

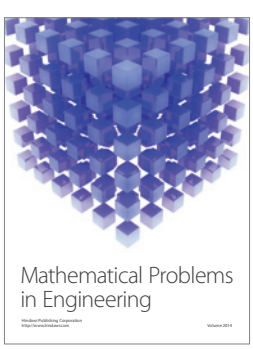

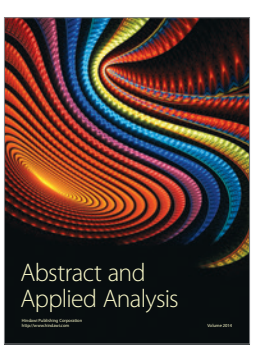

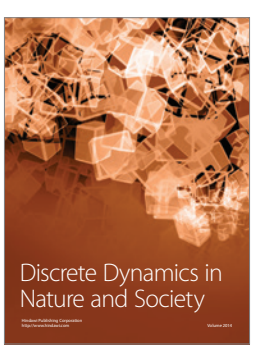

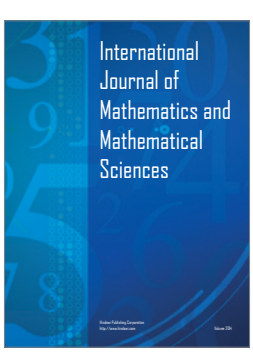

Hindawi

Submit your manuscripts at
http://www.hindawi.com